

MODE I FRACTURE TOUGHNESS PREDICTION AS A FUNCTION OF TEMPERATURE FOR A HIGH TEMPERATURE EPOXY ADHESIVE

Mariana D. Banea ^a, Lucas F. M. da Silva ^b and Raul D. S. G. Campilho ^c

^a *Unidade de Concepção e Validação Experimental, Instituto de Engenharia Mecânica (IDMEC), 4200-465, Porto, Portugal, mbanea@fe.up.pt, <http://paginas.fe.up.pt/idmec/ucve/index.html>*

^b *Departamento de Engenharia Mecânica, Faculdade de Engenharia, Universidade do Porto, Rua Dr. Roberto Frias, 4200-465 Porto, Portugal, lucas@fe.up.pt, <http://www.fe.up.pt/>*

^c *Faculdade de Economia e Gestão, Universidade Lusófona do Porto, Rua Augusto Rosa, 24, 4000-098 Porto, Portugal, raulcampilho@hotmail.com, <http://www.ulp.pt/>*

Keywords: High temperature adhesives, fracture toughness, cohesive zone models.

Abstract. In this work, the Double Cantilever Beam (DCB) test is analysed in order to evaluate the effect of the temperature on the adhesive mode I fracture toughness of a high temperature epoxy adhesive. Cohesive zone models, in which the failure behaviour is expressed by a bilinear traction–separation law, have been used to define the adhesive behaviour and to predict the adhesive load–displacement curves as a function of temperature. The simulation response for various temperatures matched the experimental results very well. It is shown that at temperatures below the glass transition temperature (T_g), the fracture toughness, G_{Ic} , is relatively insensitive to temperature, while above T_g (at 200°C) a drastic decrease in fracture toughness was observed.

1 INTRODUCTION

In the last years, there has been a growing requirement, particularly in the aerospace industry, for adhesives to withstand high temperatures. The adhesives used in structural high temperature aerospace applications must operate in extreme environments. These adhesives have to maintain their mechanical properties at the intended service temperature and to maintain their structural integrity (resist thermal breakdown at elevated temperature). Adhesive systems that meet some of these requirements include: epoxies (having high strength and temperature resistance), silicones (excellent sealant for low stress applications, high degree of flexibility and very high temperature resistance), phenolics, polyimides, bismaleimides and ceramic adhesives.

As is known, adhesive strength generally shows temperature dependence. Studies that present experimental results of adhesive joints with structural adhesives (especially epoxies) as a function of temperature generally show a decrease in strength with increasing and decreasing temperatures (Banea and da Silva, 2010; da Silva and Adams, 2005). At high temperatures this is due to the low adhesive strength, while at low temperatures the high thermal stresses and the brittleness of the adhesive are the origin of such behaviour. Similarly, the fracture toughness is expected to show temperature dependence.

Several investigators addressed the determination of the fracture toughness in tension or shear of thin adhesive layers in adhesively-bonded assemblies, but these studies are often limited to room temperature testing. Melcher and Johnson (2007) studied the Mode I fracture toughness of an adhesively bonded composite-composite joint in a cryogenic environment. They observed a substantial decrease in the fracture toughness at cryogenic temperature compared to room temperature. Banea *et al.*, (2010a) studied the pure mode I fracture toughness for adhesive joints bonded with a high temperature RTV silicone adhesive, over a wide range of temperatures (from RT to +260°C) showing that the fracture toughness and the traction–separation laws exhibit temperature dependence. Recently, Carlberger *et al.* (2009) showed in an experimental study that the fracture toughness is fairly unaffected by the temperature, from –40°C to +80°C, (the T_g of the epoxy adhesive investigated is +90°C) and the peak stress in peel loading decreased monotonically with increasing temperature in this temperature range. However, relatively only limited data are available relative to the critical strain energy release rate at low or high temperatures.

Cohesive zone models (CZMs) are now widely used to simulate fracture processes of different material systems and numerous CZM models have been presented in the literature (Needleman, 1987; Tvergaard and Hutchinson, 1992). The key concept of CZM is that the fracture process zone (FPZ) can be described by a traction–separation law relating stresses and relative displacements between the crack faces, thus simulating the gradual degradation of the material properties. As a result, a second fracture parameter, the cohesive strength, is introduced in addition to the fracture toughness. The shape of the softening law can also be adjusted to conform to the behaviour of the material it is simulating.

A few number of techniques has been used in the past to define the traction separation laws for adhesive layers, either brittle or ductile. The most common one relies on iterative comparisons between experimentally measured data and the respective numerical predictions considering a precise description of the experimental geometry and approximate cohesive laws with a parameterized shape, established based on the typical behaviour of the material that the law is simulating. Using this technique, the value of fracture toughness, which corresponds to the plateau value of the respective *R*-curve of the fracture characterization test, is used as an input parameter in the numerical model. These models also include typical values for the cohesive strength. A few numerical iterations must be performed until a good

accuracy between the experimental and numerical data is obtained. Examples of the experimental data used for fitting are the R -curves (Flinn *et al.*, 1993), the crack opening profile (Mello and K.M. Liechti, 2006), and most typically the P - δ curve (Li *et al.*, 2005). The direct method is also available, allowing the extraction of the cohesive law of an adhesive layer directly from the measured data from the experiments without requiring such a laborious numerical analysis (Pandya and J. G. Williams, 2000). In this method, the damage evolution across the width of the specimens has to be uniform, which is typically difficult to achieve. The direct method is based on the simultaneous measurement of the J -integral and the end-opening (normal or shear) of the cohesive zone. This has been successfully employed in the extraction of traction–separation laws for adhesive bonds (Sørensen, 2002; Zhu *et al.*, 2009) and fiber-reinforced composites (Sørensen and Jacobsen, 2003).

In this work, the Double Cantilever Beam (DCB) test is analysed in order to evaluate the effect of the temperature on the adhesive mode I fracture toughness of a high temperature epoxy adhesive. Cohesive zone models, in which the failure behaviour is expressed by a bilinear traction–separation law, have been used to define the adhesive behaviour and to predict the adhesive P - δ curves as a function of temperature. From the numerical simulations, the parameters that describe the bilinear CZM are determined.

2 EXPERIMENTAL

The adhesive used was a one-component high temperature paste epoxy adhesive XN1244, supplied by Nagase ChemteX (Japan).

The DCB specimen geometry and the loading are shown in Figure 1.

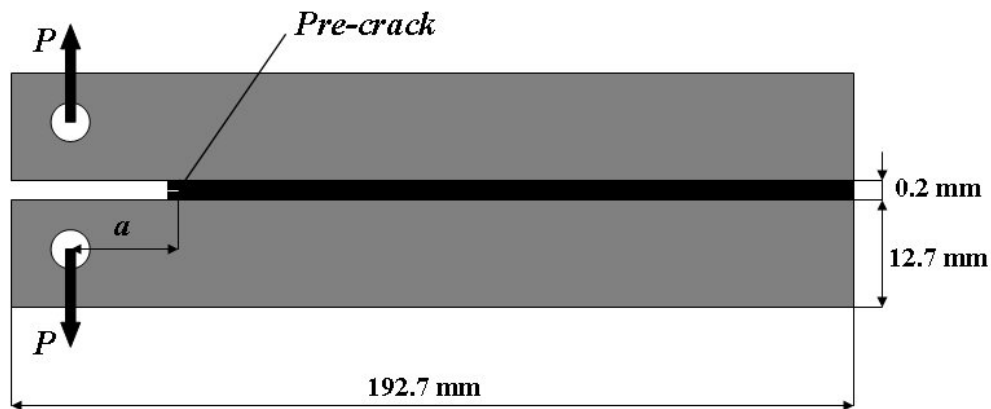


Figure 1: DCB specimen geometry

A key parameter in the testing of adhesive joints is the T_g of the adhesive. When the adhesively bonded joints are tested below this temperature, the adhesive will behave like a low-strain rigid material while above this temperature it will have a more rubber-like behaviour. The glass transition temperature of the XN1244 adhesive, obtained by dynamical mechanical analysis (DMA) method is approximately 155°C.

Testing has been undertaken to determine the material properties of the XN1244 adhesive. Table 1 summarizes the mechanical properties, which will be subsequently used for the finite element simulations. Figure 2 illustrate representative XN1244 adhesive tensile stress-strain curves as a function of temperature obtained from tensile tests, which show a decrease in XN1244 adhesive strength with increasing temperature and an increase in the ductile response

of the adhesive. The characterization of the mechanical properties of XN1244 adhesive has been described in more detail elsewhere (Banea *et al.* 2010b).

Property	RT	100°C	150°C	200°C
Young's modulus, E [GPa]	5.87 ± 0.33	4.17 ± 0.89	0.07 ± 0.01	0.04 ± 0.02
Poisson's ratio, ν^*	0.35	0.35	0.35	0.35
Tensile strength, [MPa]	68.23 ± 5.06	45.16 ± 3.48	6.49 ± 0.86	1.44 ± 0.17
Tensile failure strain, [%]	1.56 ± 0.22	1.92 ± 0.42	13.71 ± 1.46	3.33 ± 0.2

* Manufacturer's data

Table 1: Properties of the adhesive XN1244

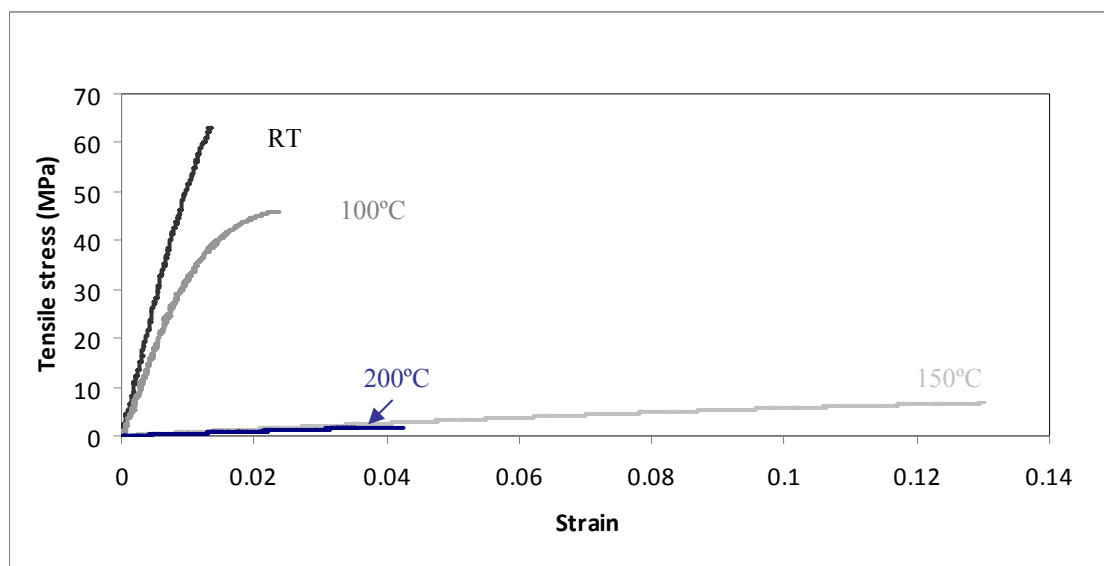


Figure 2: Representative XN1244 adhesive tensile stress-strain curves as a function of temperature

Hard tool steel DIN 40CrMnMo7 substrates were used for the DCB specimens, in order to assure an elastic behaviour of the adherends. The mechanical properties of the tool steel DIN 40CrMnMo7 are provided by supplier as follow: Yield Stress of 930 [MPa] and Young's modulus, $E=205$ [GPa].

Representative experimental P - δ curves of the DCB specimens obtained in (Banea *et al.* 2010b) at each temperatures are presented in Figure 3. The slopes and maximum loads were almost identical between RT and 100°C, but a slightly increase in displacement can be seen at 100°C. The maximum load slightly decreased at 150°C, while at 200°C, a dramatic drop in maximum load and displacement was observed.

The critical fracture energy in mode I was evaluated using the Corrected Beam Theory (CBT), Compliance-Based Beam Method (CBBM) and the Compliance Calibration Method (CCM) methods presented in (Banea *et al.* 2010b). The effect of temperature on the fracture toughness, G_{Ic} , is presented in Figure 4. At 100°C the fracture toughness, G_{Ic} , of the adhesive slightly increased (by approximately 10%). This can be explained by the fact that, as the temperature increases, the strength decreases but the ductility increases giving an additional plastic deformation at the crack tip, hence an increase in toughness. At 150°C, G_{Ic} is slightly

lower indicating the vicinity to the T_g . However, a drastic drop in fracture toughness was observed at 200°C. This was expected as the testing temperature overpasses the T_g of the adhesive.

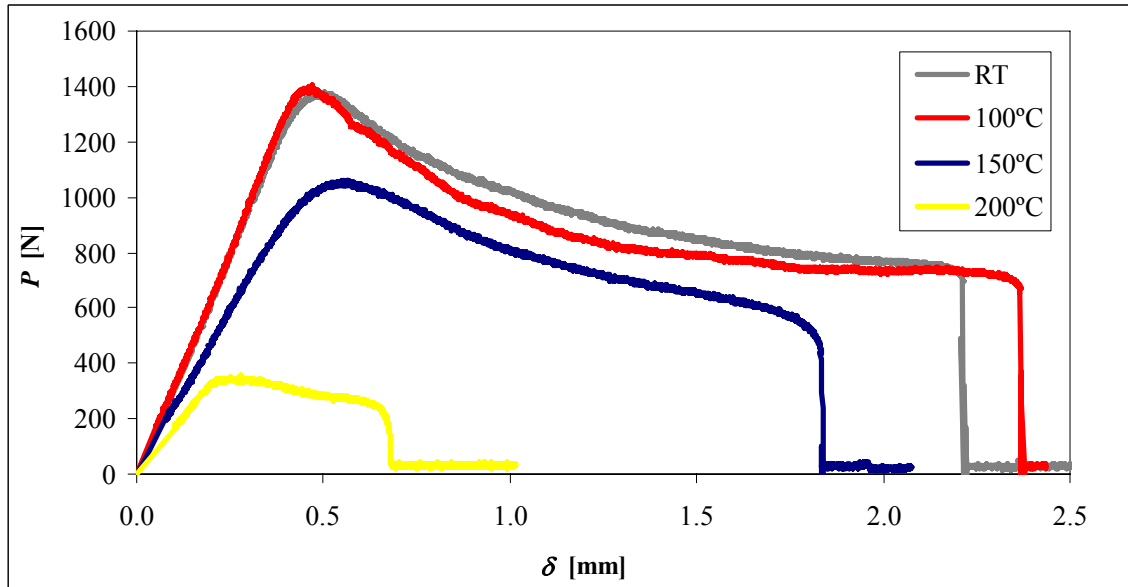


Figure 3: Representative experimental P - δ curves of the DCB specimens as a function of temperature.

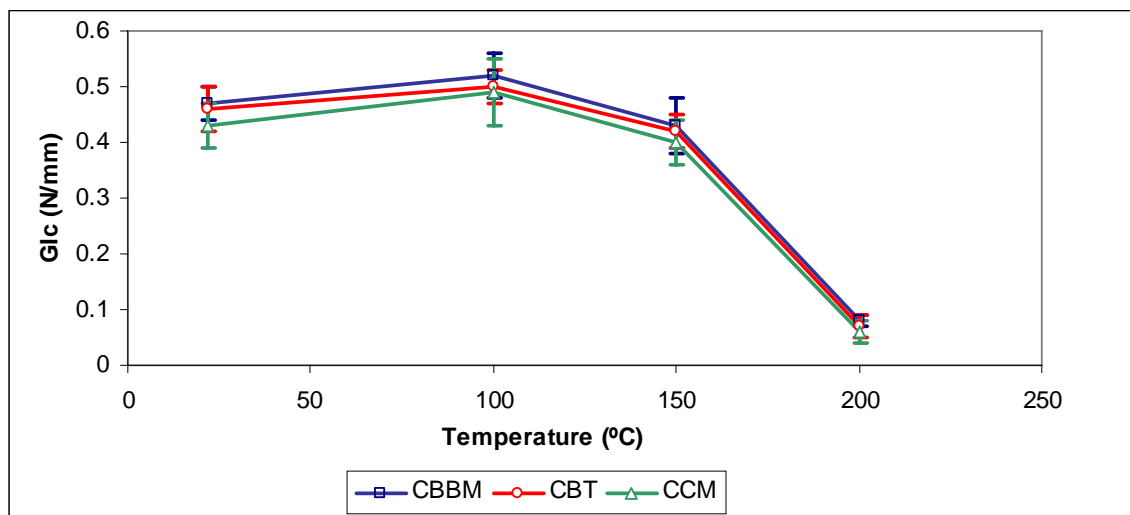


Figure 4: Fracture toughness G_{Ic} as a function of temperature

3 NUMERICAL MODELLING

A numerical analysis of the DCB joints as a function of temperature was performed in the commercial FEM package ABAQUS[®] to assess the viability of its CZM formulation, discussed further in terms of generic principles, in reproducing the experimental tests performed. The numerical analysis was carried out using non-linear geometrical considerations using the material properties defined in Table 2. The deformed shape of the DCB specimen during damage propagation and the applied boundary and loading conditions

are shown in Figure 5. The specimen arms were modelled with plane-strain 8-node quadrilateral solid finite elements (CPE8 from ABAQUS[®]) and the adhesive was modelled with 6-node cohesive elements, including the bilinear mixed mode CZM. Twelve solid finite elements were used through-thickness in each arm, with a more refined mesh near the adhesive region. The meshes were constructed taking advantage of the automatic meshing capabilities of ABAQUS[®], from a manual seeding procedure that included biasing effects from the loading points towards the crack tip, where large stress gradients are expected. In the damage propagation region a more refined mesh was used, considering 0.20 mm length elements. The applied boundary conditions consisted on clamping the lower edge node of the lower arm, and applying a vertical displacement and horizontally restraining the upper edge node of the upper arm (Figure 5).

Temperature(°C)	G_n^c [N/mm]	t_n^c [MPa]	E [MPa]	G[MPa]
RT	0.47	68	5872	2260
100	0.50	45	4173	1605
150	0.42	6.5	72	28
200	0.07	1.4	40	16

Table 2: The adhesive material properties used for simulations

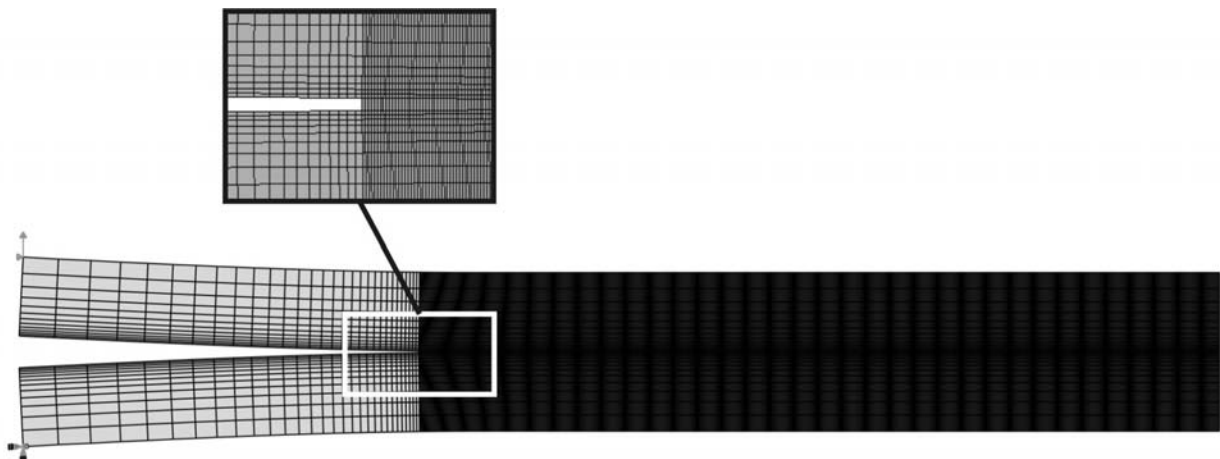


Figure 5: Deformed shape of the DCB specimen during propagation, with boundary and loading conditions

3.1 Cohesive zone model

CZM's model the elastic loading, initiation of damage and propagation due to local failure within a material predicting the full description of the structures damage process up to failure. CZM's are based on a relationship between stresses and relative displacements between initially superimposed nodes of the cohesive elements (Figure 6), simulating the elastic behaviour up to a peak load and subsequent softening, to simulate a gradual degradation of material properties. Generically speaking, the shape of the softening laws can be adjusted to conform to the behaviour of the material or interface they are simulating (Campilho *et al*, 2008).

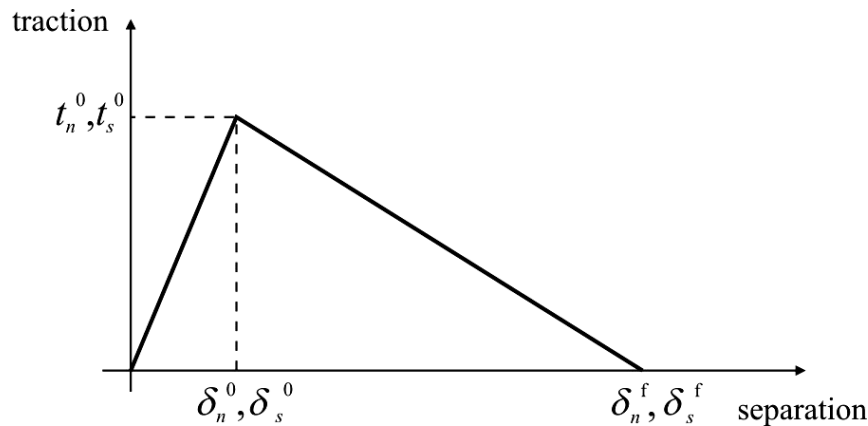


Figure 6: Traction-separation law with linear softening available in ABAQUS®

The areas under the traction-separation laws in each mode of loading (tension and shear) are equalled to the respective fracture energy. Under pure mode, damage propagation occurs at a specific integration point when the stresses are released in the respective traction-separation law. Under mixed mode, energetic criteria are often used to combine tension and shear (Campilho *et al*, 2008), thus simulating the typical mixed mode behaviour inherent to bonded assemblies. In this work, a continuum-based approach was considered to model the finite thickness of the adhesive layer. The cohesive layer is assumed to be under one direct component of strain (through-thickness) and one transverse shear strain, which are computed directly from the element kinematics. The membrane strains are assumed as zero, which is appropriate for thin and compliant layers between stiff adherends. The traction-separation law assumes an initial linear elastic behaviour followed by linear evolution of damage. Elasticity is defined by an elastic constitutive matrix relating stresses and strains across the interface (ABAQUS®):

$$\mathbf{t} = \begin{Bmatrix} t_n \\ t_s \end{Bmatrix} = \begin{bmatrix} K_{nn} & K_{ns} \\ K_{ns} & K_{ss} \end{bmatrix} \cdot \begin{Bmatrix} \varepsilon_n \\ \varepsilon_s \end{Bmatrix} = \mathbf{K}\boldsymbol{\varepsilon} \quad (1)$$

The matrix \mathbf{K} contains the stiffness parameters of the adhesive layer, given by the quotient between the relevant elastic modulus and the adhesive thickness. A suitable approximation for thin adhesive layers is provided with $K_{nn}=E$, $K_{ss}=G$, $K_{ns}=0$; E and G are the longitudinal and transverse elastic moduli (Campilho *et al*, 2008). Damage initiation can be specified by different criteria. In this work, the quadratic nominal stress criterion was considered for the initiation of damage, already shown to give accurate results, expressed as (ABAQUS®):

$$\left\{ \frac{\langle t_n \rangle}{t_n^0} \right\}^2 + \left\{ \frac{t_s}{t_s^0} \right\}^2 = 1 \quad (2)$$

t_n^0 and t_s^0 represent the pure mode (normal or shear, respectively) peak values of the nominal stress. $\langle \rangle$ are the Macaulay brackets, emphasizing that a purely compressive stress state does not initiate damage. After the peak value in Figure 6 is attained, the material stiffness is degraded under different possible laws, depending on the material to be simulated. For brittle materials such as the XN1244, a linear softening law is sufficiently appropriate (Alfano, 2006). Complete separation is predicted by a linear power law form of the required

energies for failure in the pure modes:

$$\frac{G_n}{G_n^c} + \frac{G_s}{G_s^c} = 1. \quad (3)$$

The quantities G_n and G_s relate to the work done by the traction and corresponding relative displacements in the normal and shear directions, whilst the relating critical fracture energies required for pure mode failure are given by G_n^c and G_s^c for normal and shear loadings, respectively.

The shape of the traction–separation law for each mode is defined as a bilinear model. Therefore, only two parameters need to be determined (G_n^c and t_n^0), typically determined experimentally.

The t_n^0 can also be extracted by comparing numerical predictions from cohesive-zone simulations to the results of experimental tests.

The maximum relative displacement, δ_n^f , for which complete failure occurs, is obtained by equating the area under the softening curve (the triangle of Figure 6) to the respective critical fracture energy (Eq.4).

$$G_n^c = \frac{1}{2} t_n^0 \delta_n^f \quad (4)$$

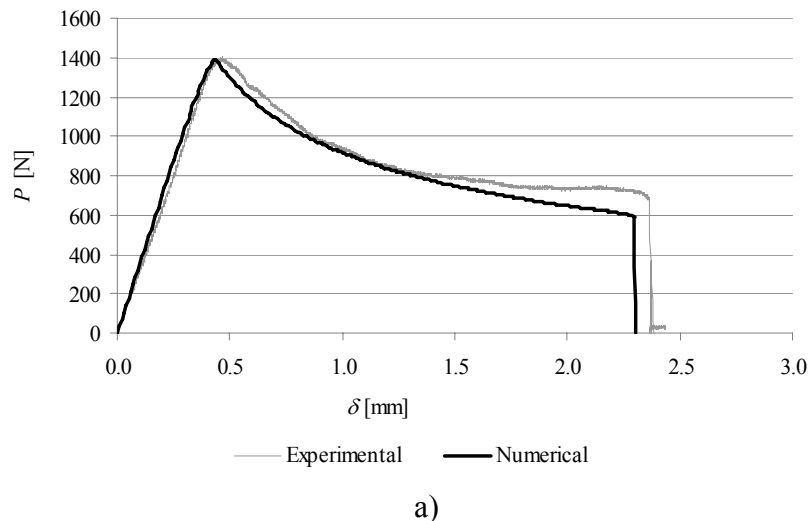
The values introduced in ABAQUS[®] for the simulation of damage in the adhesive layer are listed in Table 2.

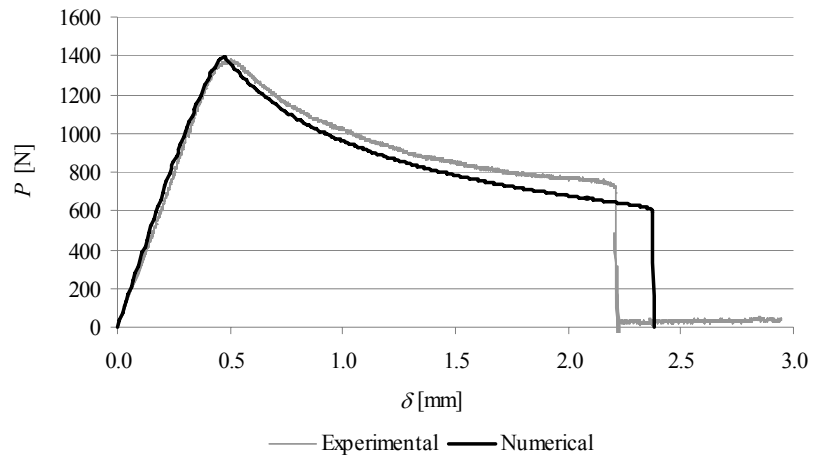
4 NUMERICAL RESULTS AND DISCUSSION

4.1 Comparison with the experiments

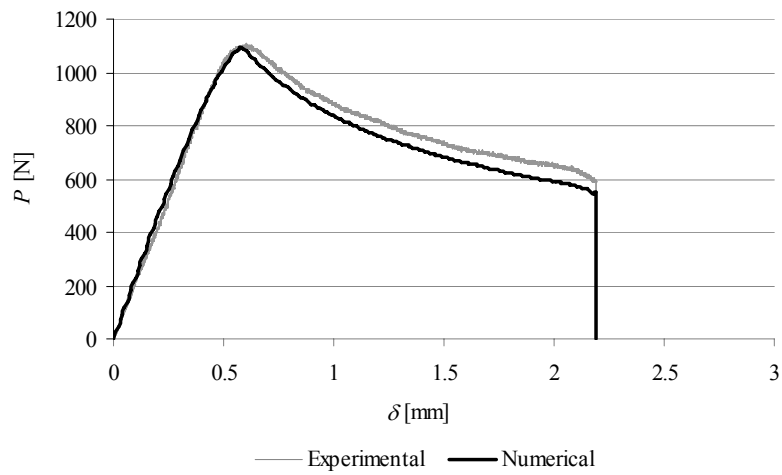
The determination of G_{Ic} and t_n^0 for various temperatures were done experimentally from the DCB tests and tensile tests, respectively. The remaining cohesive parameters are obtained with an inverse method, fitting the numerical P – δ curves with the experiments and allowing complete fracture characterization of the adhesive as a function of temperature in pure mode I. This method consisted of inputting each G_{Ic} and t_n^0 in the respective DCB model, as a function of temperature.

In Figure 7, experimental and numerical P – δ curves of the DCB specimens at RT (a), 100°C (b), 150°C (c) and 200°C (d) can be seen. The simulation response for various temperatures matches the experimental results very well.

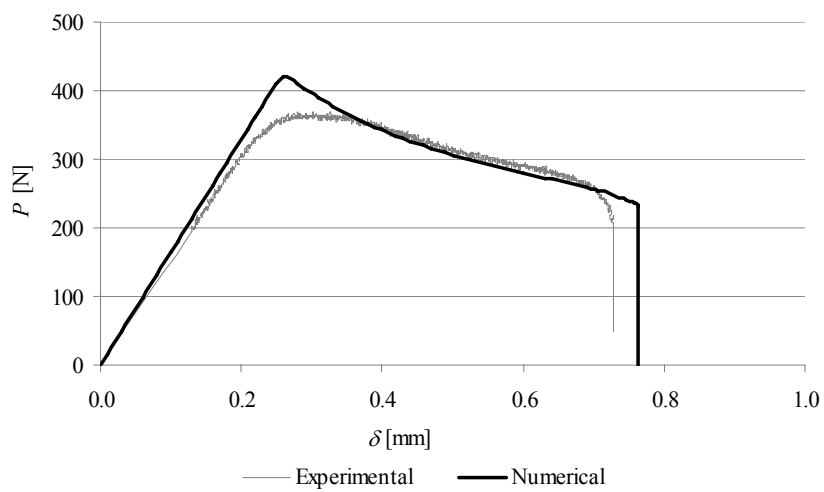




b)



c)



d)

Figure 7: Experimental and numerical P - δ curves of the DCB specimens at RT (a), 100°C (b), 150°C (c) and 200°C (d).

Experimental and numerical R -curves for one specimen at RT, 100°C, 150°C and 200°C are presented in Figure 8. An excellent agreement was found between the experimental and numerical R -curves.

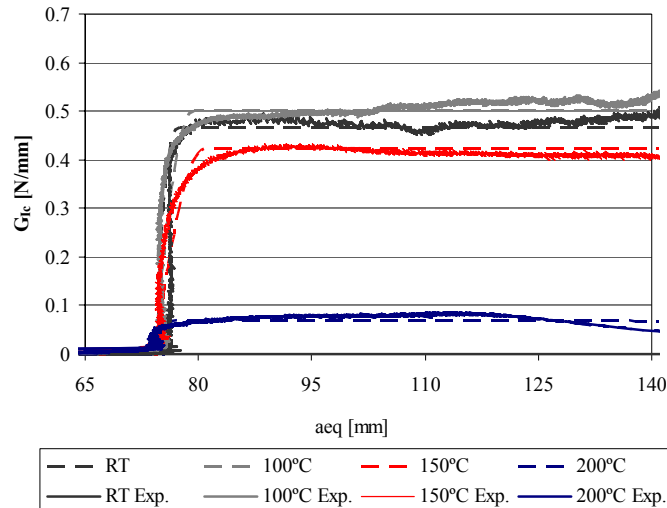


Figure 8: Experimental and numerical R -curves of one DCB specimen as a function of temperature.

5 CONCLUSIONS

The goal of this study was to determine the appropriate cohesive laws for pure mode I, as the first step in developing a methodology for design-level predictions of the effect of temperature on the performance of structural adhesive joints for high temperature applications.

Cohesive zone models have been used to characterize the adhesive behaviour and to predict the adhesive P - δ curves as a function of temperature. The simulation response for various temperatures matches the experimental results very well. From the numerical simulations, the parameters that describe the bilinear CZM were determined. The fracture toughness was found to be essentially temperature independent below T_g . Moreover, a drastic drop in fracture toughness was observed at 200°C, when the T_g of the adhesive was overpassed. The cohesive strength decreases as the temperature increase.

ACKNOWLEDGEMENTS

The authors would like to thank the Portuguese Foundation for Science and Technology for supporting the work presented here, through the individual grant SFRH/BD/61880/2009 and through the research project PTDC/EME-PME/67022/2006, and Nagase ChemteX (Japan) for supplying the adhesive.

REFERENCES

- ABAQUS® HTML Documentation, Dassault Systemes, 2009.
- Alfano, G. On the influence of the shape of the interface law on the application of cohesive-zone models. *Composites Science and Technology*, 66:723-730, 2006.
- Banea, M. D. and Da Silva, L. F. M., The effect of temperature on the mechanical properties of adhesives for the automotive industry. *Proceedings of the Institution of Mechanical Engineers, Part L: Journal of Materials: Design and Applications*, 224:51-62, 2010.

- Banea M.D., da Silva, L.F.M. and Campilho RDSG, Temperature Dependence of the Fracture Toughness of Adhesively Bonded Joints, *Journal of Adhesion Science and Technology*, 24:2011–2026, 2010a.
- Banea, M.D., da Silva, L.F.M. and Campilho, R.D.S.G., Effect of temperature on tensile strength and mode I fracture toughness of a high temperature epoxy adhesive, *Journal of Adhesion Science and Technology*, submitted, 2010b.
- Campilho, R. D. S. G., De Moura, M. F. S. F. and Domingues, J. J. M. S., Using a cohesive damage model to predict the tensile behaviour of CFRP single-strap repairs. *International Journal of Solids and Structures*, 45:1497-1512, 2008.
- Carlberger, T., Biel, A. and Stigh, U. Influence of temperature and strain rate on cohesive properties of a structural epoxy adhesive. *International Journal of Fracture*, 155:155-166, 2009.
- Da Silva, L. F. M. and Adams, R. D., Measurement of the mechanical properties of structural adhesives in tension and shear over a wide range of temperatures. *Journal of Adhesion Science and Technology*, 19:109-141, 2005.
- Flinn, B. D., Lo, C. S., Zok, F. W. and Evans, A. G., Fracture Resistance Characteristics of a Metal-Toughened Ceramic. *Journal of the American Ceramic Society*, 76:369-375, 1993.
- Gustafson, P. A. and Waas, A. M. The influence of adhesive constitutive parameters in cohesive zone finite element models of adhesively bonded joints. *International Journal of Solids and Structures*, 46:2201-2215, 2009.
- Li, S., Thouless, M. D., Waas, A. M., Schroeder, J. A. and Zavattieri, P. D. Use of mode-I cohesive-zone models to describe the fracture of an adhesively-bonded polymer-matrix composite. *Composites Science and Technology*, 65:281-293, 2005.
- Melcher, R. J. and Johnson, W. S., Mode I fracture toughness of an adhesively bonded composite-composite joint in a cryogenic environment. *Composites Science and Technology*, 67:501-506, 2007.
- Mello, A. W. and Liechti, K. M., The Effect of Self-Assembled Monolayers on Interfacial Fracture. *Journal of Applied Mechanics*, 73:860-870, 2006.
- Needleman, A., A Continuum Model for Void Nucleation by Inclusion Debonding. *Journal of Applied Mechanics*, 54:525-531, 1987.
- Pandya, K. C. and Williams, J. G., Measurement of cohesive zone parameters in tough polyethylene, *Polymer Engineering and Science* 40(8):1765-1776, 2000.
- Sørensen, B. F., Cohesive law and notch sensitivity of adhesive joints. *Acta Materialia*, 50:1053-1061, 2002.
- Sørensen, B. F. and Jacobsen, T. K., Determination of cohesive laws by the J integral approach. *Engineering Fracture Mechanics*, 70:1841-1858, 2003.
- Sun, C., Thouless, M. D., Waas, A. M., Schroeder, J. A. and Zavattieri, P. D., Ductile-brittle transitions in the fracture of plastically deforming, adhesively bonded structures. Part II: Numerical studies. *International Journal of Solids and Structures*, 45:4725-4738, 2008.
- Tvergaard, V. and Hutchinson, J. W., The relation between crack growth resistance and fracture process parameters in elastic-plastic solids. *Journal of the Mechanics and Physics of Solids*, 40:1377-1397, 1992.
- Zhu, Y., Liechti, K. M. and Ravi-Chandar, K., Direct extraction of rate-dependent traction-separation laws for polyurea/steel interfaces. *International Journal of Solids and Structures*, 46:31-51, 2009.